Acta Cryst. (1995). B**51**, 592–603

Diffuse Scattering from Disordered Crystals

BY F. FREY

Institut für Kristallographie, LMU, Theresienstrasse 41, 80333 *München, Germany*

(*Received* 21 *July* 1994; *accepted* 23 *February* 1995)

Abstract

General aspects of disorder diffuse scattering are discussed. Diffuse scattering of crystals is due to deviations in space and/or time from an average structure of strict long-range order, where long-range order refers to three-dimensional translational periodicity. The iodine chain compound $E_2PI_{1.6}$ serves as an example where the one-dimensional iodine substructure was studied by a quantitative analysis of extended diffuse layers. With this example general problems of a structure analysis by means of diffuse data are discussed. In urea inclusion compounds complicated order/disorder processes and subsequent phase transitions are related to longitudinal and lateral ordering within and between the urea host and the *n*-paraffin guest substructure. Combined X-ray and neutron methods help to clarify the static/dynamic origin of the diffuse scattering *viz.* disorder phenomena. Zirconia, ZrO_2 doped with various metal oxides, exhibits defect structures which decisively determine material properties. The defect structure can be interpreted by a quantitative analysis of diffuse data in the frame of a model of correlated microdomains. Diffuse scattering of quasicrystals (q.c.) is due to breaking of translational periodicity in *N*-dimensional space ($N > 3$), including fluctuations of sizes and shapes of $(N-3)$-dimensional 'hyperatoms'. Diffuse scattering of the (q.c.) decagonal phase AlNiCo indicates disorder with respect to one-dimensional translational and two-dimensional q.c. order. In particular, super-ordering and disordering within the q.c. arrangement are due to periodically ordered segments. Future trends of disorder diffuse scattering work are outlined.

1. Disorder diffuse scattering: general remarks

Diffuse scattering from crystals is due to deviations in space and/or time from an average structure of strict long-range order. Long-range order refers to three-dimensional translational periodicity of atoms or molecules or larger structural units. As long as such an averaged structure can be defined, the scattering density can be divided into

$$\rho(r) = \langle\rho(r)\rangle + \Delta\rho(r),$$

where the definition indicates that $\langle\Delta\rho(r)\rangle = 0$, $\langle\rho(r)\rangle$ is the projection of all unit cells into a single one repeated strictly periodically in space (divided by the number of cells), $\Delta\rho(r)$ denotes fluctuations in space and/or time. The intensity of the scattered beam $I_{\rm tot}$ is given by the Fourier transform of

$$\rho(r) \otimes \rho(r) = \langle\rho(r)\rangle \otimes \langle\rho(r)\rangle + \Delta\rho(r) \otimes \Delta\rho(r),$$

where $\otimes$ denotes convolution. Thus, the total intensity $I_{\rm tot}$ can be divided into a Bragg component I_B and a diffuse component I_D

$$I_{\rm tot} = I_B + I_D = |\langle F(Q)\rangle|^2 + [\langle|F(Q)|^2\rangle - |\langle F(Q)\rangle|^2].$$

Both components contain information regarding an underlying disorder problem. The average structure

$$\langle\rho(r)\rangle = \sum n_k \delta(r - r_k) \otimes \rho_k(r) \otimes pdf_k(u)$$

and its corresponding Fourier transform (structure factor)

$$\langle F(Q)\rangle = \sum n_k \exp\{iQr_k\} f_k(Q) T_k(Q)$$

may be analysed in terms of occupation factors n_k and probability density functions $pdf_k(u)$, which result from the projections of statically or dynamically displaced atoms into one cell (*cf.* above). $\rho_k(r)$ denotes the scattering density of atom k and $pdf_k(u)$ is the Fourier transform of the (generalized) temperature factor

$$T_k(Q) = \int pdf_k(u) \exp\{iQu\} du.$$

The more direct way to solve a disorder problem is to analyse the diffuse intensity component I_D, which corresponds to the Fourier transform of the deviations from an average structure. There is, however, no general theory equally well applicable to the various order/disorder problems such as competing ordering in compounds with weakly bound substructures, domains, super/modulated structures, orientational disorder, lamellar ordering, turbostratic structures *etc.* There are also problems which cannot be treated adequately by the separation into Bragg and diffuse components. Different disorder problems are discussed and corresponding solutions are outlined, *e.g.* Jagodzinski & Frey (1993) and references therein. Review articles about disorder diffuse scattering are also given in *e.g.* Welberry (1985), Jagodzinski (1987), and Welberry & Butler (1994).

A specific disorder phenomenon may depend on the prehistory of a sample or on external parameters such as temperature or pressure, and may be time-dependent. The

©1995 International Union of Crystallography
Printed in Great Britain – all rights reserved

disordering may be inhomogeneous and related to microstructures in the sample, and may depend on particle size effects or strains. Beyond crystallographic structural aspects, investigations of disorder are therefore related to basic problems in solid-state physics and solid-state chemistry. On the other hand, many crystals or, more generally, solid-state properties, such as optical properties, hardness of alloys and ionic conductivity, are dominated by defects and structural disorder. Diffuse scattering investigations are therefore a tool in materials science. Order/disorder phenomena are related to growth conditions, *e.g.* chemical environment, pressure, time *etc.* Because most of the crystalline materials from the earth, *i.e.* minerals, are disordered, their study allows basic questions in the geosciences to be answered.

Disorder diffuse scattering from quasicrystals is even more exotic than from 'ordinary' crystals. Here we have to discuss, in principle, the breaking of translational periodicity in N-dimensional space ($N > 3$) and, in addition, to consider fluctuations of sizes and shapes of decorated ($N - 3$)-dimensional hyperatoms. Again, there is no general disorder theory of quasicrystals and experimental work is very rare. Similarly one can try to separate the total scattering into Bragg and diffuse components, but now the Fourier transform of the average structure has to be reconsidered. The Bragg peaks may now be indexed by components in an external and an internal subspace (or parallel and perpendicular subspace, respectively; see *e.g.* Janot, 1992). Correspondingly, the intensity dependence may be different in both subspaces and new types of disorder may occur, such as phasons, phason strains and others. Moreover, the competition between periodic and aperiodic ordering leads to complicated intermediate states, such as approximants or complicated twin structures. An overview is given, for example, by Goldman & Kelton (1993). On the other hand, diffuse scattering contributions in quasicrystals are of key importance if discussing fundamental questions such as the stability and perfectness of a quasicrystal. As stated by Jaric & Nelson (1988), a perfect quasicrystal exhibits δ-function peaks and no diffuse scattering – which is common knowledge in traditional crystallography. In other words, more or less disordered quasicrystals exhibit sharp peaks as long as a long-range ordered average structure or substructure may be defined and the sharpness of reflections is neither a correct nor a sufficient argument in favour of a thermodynamical stability of a q.c. phase.

Some general characteristics of diffuse scattering of any kind should be mentioned in this short overview. Diffuse intensities are generally weaker than Bragg scattering by several orders of magnitude. Note, however, that diffuse scattering integrated over a reciprocal cell may be comparable or even exceed the intensity of a Bragg reflection. Neglecting diffuse intensity therefore means wasting information. In reciprocal space diffuse scattering is usually anisotropically distributed. Therefore, specific experimental techniques and detailed resolution considerations are necessary. Different disorder models can be distinguished by the dependence of the diffuse scattering on the scattering vector **Q**, *i.e.* by exploring a large area of the reciprocal space. This is time consuming and always in conflict with the demand of good resolution. In the following, examples are given to demonstrate the usefulness and even uniqueness of diffuse scattering investigations to analyse the disorder problem.

2. 5,10-Diethyl-5,10-dihydrophenazinium iodide: structure analysis from diffuse data

The title compound, briefly $E_2PI_{1.6}$, consists of two substructures (Endres *et al.*, 1979): an almost tetragonal framework (slight monoclinic distortion) is built up by one-dimensional stacks of planar but tilted organic E_2P molecules (the host structure) and iodine chains embedded in channels running along the unique c axis. Both substructures interact with one another only weakly; the host period $c_o = 5.27$ Å is incommensurate with the c-spacing of the chains $c_I = 9.57$ Å. There are also only weak interactions between the I chains, which form, to a first approximation, a one-dimensional substructure. Even at low temperatures, 25–30 K, there is no complete three-dimensional ordering. The most prominent diffuse phenomenon is a set of diffuse layers perpendicular to the c^* direction (Fig. 1), the distance between the layers corresponds to the translational period along the chain units.

Assuming a system of uncorrelated linear chains, which is justified for temperatures above 200 K, a simple analysis of the l distribution of the diffuse intensities $I(l)$ in the framework of the paracrystal method (Hosemann & Bagchi, 1962) gives an asymmetry of the linear I_3-units, the mean distance between them, and the parameters of a one-dimensional distribution function h(z)

$$I(l) = |\mathcal{F}\{\rho_m(z)\}|^2 G(l),$$

where $\mathcal{F}$ denotes the Fourier transformation, $\rho_m(z)$ refers to the one-dimensional structure of the I_3-unit and $G(l)$ describes the interference function

$$G(l) = 1 + \mathbb{R}e\{H(l)/(1 - H(l)\},$$

where $H(l)$ denotes the Fourier transform of $h(z)$. Different distribution functions are discussed by Rosshirt, Frey, Boysen & Jagodzinski (1985). It turns out that the I_3-molecules have a fluid-like character within the channels. This analysis is straightforward because the heavy I atoms and the organic matrix contribute almost exclusively to the diffuse layers and to the Bragg peaks, respectively. Generally, one has to be very careful in this respect because even weak interactions usually give rise to common (super-) periodicities

and, in consequence, to mutual intensity contributions despite different 'dimensionalities' of the substructures.

A second system of diffuse layers between the main one (*cf.* Fig. 1) indicates a double superperiodicity within the chains, a pseudo-extinction rule suggests a pseudo-2_1 or -4_2 screw-like symmetry element. Different simple models were developed, which obey an overall cylindrically symmetric intensity distribution and a pseudo-extinction close to **c***. Some examples are shown in Fig. 2 (Wildgruber, 1989). Intensity calculations based on a more realistic I_3-molecule arrangement were compared with the measured intensities (see below), including the lateral dependence perpendicular to the c^* axis. Analytical expressions, as well as expansions in powers of Fourier–Bessel functions, were used. Due to the relatively small accessible $\mathbf{Q}_R$-range, ≤ 2.5 Å^{-1}, where $\mathbf{Q}_R$ is the radial component of the scattering vector, there is no significant difference if the expansion is limited to the fifth order. None of the models, however, allowed a satisfactory simultaneous quantitative refinement of all diffuse layers. No strict screw-like symmetry element exists. In consequence, structural parameters of the iodine chains have to be refined without any assumption of the molecular configurations. This means that all degrees of freedom have to be represented by free structural parameters, *i.e.* asymmetric bond lengths, translations and rotations of the molecules with respect to the *c* axis, *e.g.* tilting, kinking or skew orientations. Therefore, a structure analysis of three-dimensional molecules was performed from pure diffuse data recorded at low temperatures (25–30 K), because the fluid-like character along **c** is lost at low temperatures, a prerequisite for this analysis. Note, however, that a system of diffuse layers at distances $\pm m/6$ from the main layers becomes strong at low temperatures (Fig. 3) and complicates this analysis more.

Any step of a structure analysis, which is more or less routine work in conventional crystallography, must be reconsidered: (i) recording and correcting experimental data, (ii) applying classical methods of structure analysis by means of user-friendly software packages, (iii) carrying out refinement procedures by least-squares methods and by the use of well defined agreement factors, (iv) giving confidence levels and performing significance tests, and (v) giving limits of accuracy and precision. Some of the (experimental and theoretical) problems of a structure analysis from pure diffuse data will be discussed very briefly with this example.

The measurement of extended diffuse data demands the facilities of two-dimensional (area) detectors, *e.g.*

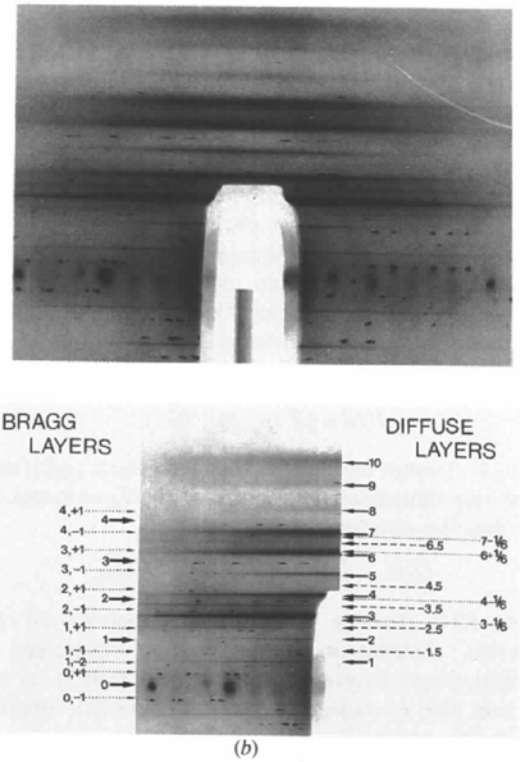

(*b*)

Fig. 1. Diffuse layer line system in $E_2PI_{1.6}$ (Wildgruber, 1989). NOROMOSIC (non-rotating monochromatic single crystal) technique, primary beam perpendicular to the *c*-axis. In (*b*) which is the same X-ray photograph with a lower exposure time, labelling of Bragg and diffuse layers is indicated. Note three systems of diffuse layers.

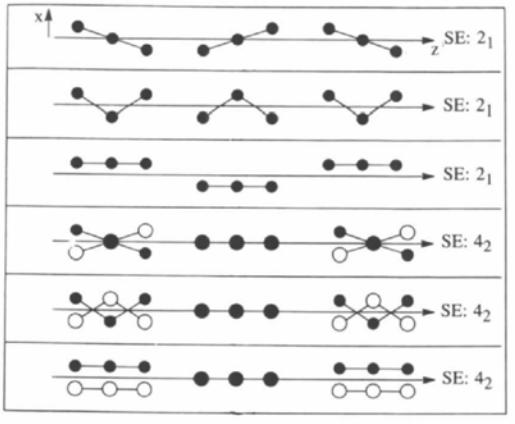

Fig. 2. Schematic picture of possible arrangements of I_3 molecules obeying a 2_1 or 4_2 symmetry.

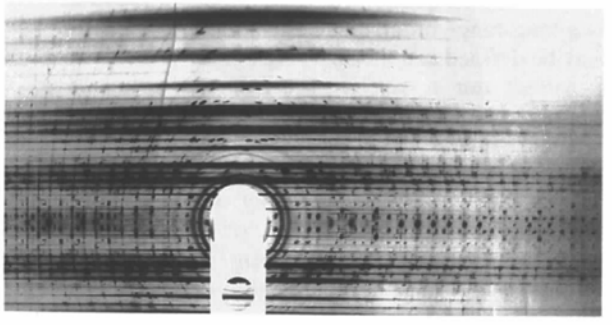

Fig. 3. Low-temperature X-ray photograph (30 K) of $E_2PI_{1.6}$ (technique as in Fig. 1). Note the enhanced intensity of the diffuse satellite layers and the additional satellite layers to the Bragg layers.

classical photographic films with subsequent microdensitometer scanning, image plates or electronic multiwire position-sensitive detectors. Besides the problem of handling an enormous amount of digital data, one is faced with problems of calibrating, normalizing and weighting intensities. In the present example we used classical film techniques combined with subsequent microdensitometer scanning. After analogue-digital conversion, the correct weighting of the diffuse data must be carried out. A treatment using conventional procedures (*International Tables for Crystallography* 1985, Vol. III, p. 142) is not satisfactory (Wildgruber, 1989). The background separation/reduction is a very important but tedious procedure. It requires not only the removal of a spurious slowly varying background from the diffuse intensity distribution, but also the separation of short-range order maxima (see below) or superimposed Bragg peaks due to the host structure. In the present example we took care of such peaks by fitting different functions to match the profiles as closely as possible. Integrated intensities of the diffuse intensity distribution were obtained by sections through the layers parallel to **c*** and subsequent fitting of Gaussians (Fig. 4). Only in this way the intensities of the $\frac{1}{6}$ satellite layers could be treated adequately. Lorentz or, more generally, resolution corrections demand a very detailed consideration of the shape and extent of the diffuse intensity distribution in reciprocal space, in relation to shape and extent of the resolution volume. A detailed discussion is given elsewhere (Boysen & Adlhart, 1987; Jagodzinski & Frey, 1993). Considerable intensity gain without loss of resolution ('focusing') is sometimes possible. The absorption may vary remarkably during scanning along an extended diffuse feature. In our example the change along a diffuse layer amounts to 25%. Numerical corrections, carried out in the present example with bicubic spline functions, were therefore necessary. Performing a refinement with the corrected integrated intensities we have the problem of an adequate *R*-factor: The superposition of laterally uncorrelated I chains gives, again to a first approximation, a cylindrically averaged intensity distribution, which indicates that we have relatively smaller *R* values compared with those used in a conventional stucture refinement. Similar to the structure analysis of fibre structures, we need some knowledge about the largest likely values to judge the

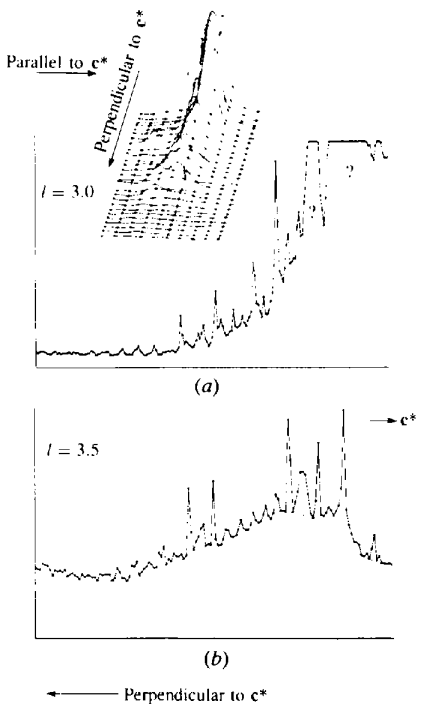

Fig. 4. Diffuse layer lines of $E_2PI_{1.6}$: The two graphs show sections along the layer line (*a*) $l = 3$ and (*b*) $l = 3.5$ (*cf.* Fig. 1), *i.e.* the sections are perpendicular to **c*** (from right to left increasing distance from **c***). The dashed lines indicate the diffuse intensity part. The inset (top) indicates the intensity integration over the diffuse layers in sections across the layers. The solid lines in this inset correspond to the dashed lines mentioned above. By this procedure diffuse intensities were separated from contaminating maxima. These integrated diffuse intensities were used for the structure analysis discussed in the text.

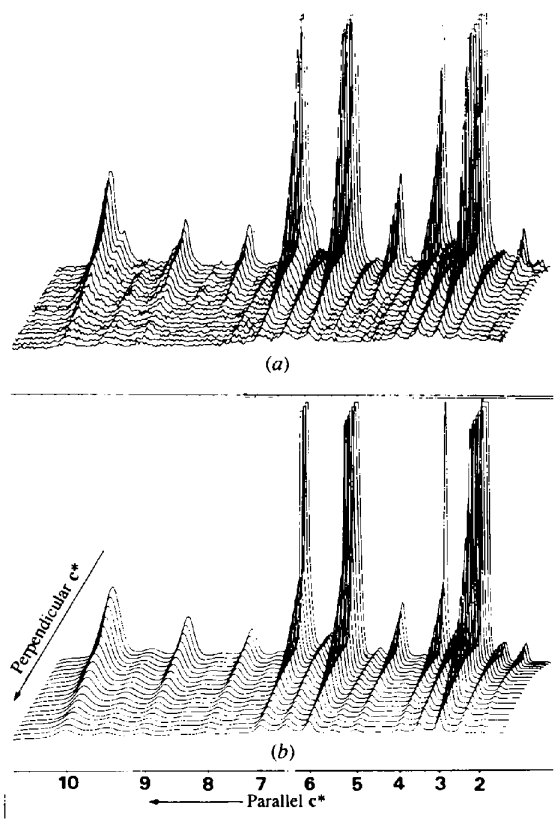

Fig. 5. Comparison of (*a*) calculated and (*b*) measured diffuse layers of $E_2PI_{1.6}$ in a perspective view. Only the main diffuse layers are indicated, increasing numbers (abscissa) indicate the increasing layer order (from right to left; *cf.* Fig. 1). Labelling 'perpendicular **c***' means parallel to the diffuse layer lines; the increasing distance from the meridian (00*l*) is indicated by the arrow head.

quality of our refinement (Stubbs, 1989; Millane, 1989). Apparently, this point must be considered separately for any specific problem. Beyond these problems with an adequate treatment of diffuse intensities, there remains the phase problem. If the disorder is unknown this problem cannot be solved (Jagodzinski, 1964) – how to find the phase of a more or less extended diffuse reflection. In consequence, Fourier methods are usually not practical.

In our example, different starting models, different types of background fitting, with and without absorption correction..., were used and the respective influence of the parameters was studied. In the refinements up to $3 \times 3 \times 6 = 36$ static parameters and two (longitudinal and lateral) overall temperature coefficients were used together with 10–15 additional parameters, taking into account the effects discussed above. A comparison between observed and calculated diffuse data is shown in Fig. 5. In this way the basic I structure at low temperatures was found to consist of six triiodide anions with individual molecular structure, *i.e.* slightly asymmetric, kinked and tilted I_3-ions. Averaged intramolecular distances were 2.88 (6) and 3.03 (5) Å, and the averaged intermolecular distance was 3.69 Å, which is lower than the van der Waals distance. An asymmetry is known from three-dimensional order I compounds in which the I_3 length exceeds 5.8 Å. The bond angles fluctuate around 177°. A further structural crystal–chemical discussion is not within the scope of this review, it should only be emphasized that, of course, the structural parameters of the I chains are affected by the interaction with the framework structure. In conclusion, it should be mentioned that the disorder problem in $E_2PI_{1.6}$ is more complicated than could be outlined here. There are modulations within all diffuse layers, *e.g.* diffuse rods, diffuse reflections, curved steaks, satellite layers to the Bragg spots with an 11-fold superperiod, which is commensurate with the sixfold superperiod of the chains (*cf.* Fig. 3). Therefore, the treatment by isolated substructures is a first approximation only.

3. Urea inclusion compounds $OC(NH_2)_2 + C_nH_{2n+2}$: disorder and phase transitions

This class of structures shows some similarity to the iodine chain compound discussed in the previous section. A hexagonal framework of urea molecules with honeycomb-like cross-section and open channels along the unique c axis includes n-alkane molecules (and other molecules which will not be considered here) within these channels. The diffuse scattering phenomena and the corresponding disorder problems, however, are much more complicated than those observed in the iodine compound. Disorder phenomena are investigated by several groups, *e.g.* by Harris (1993) and Fukao (1994). The disordering is related to the atoms within one alkane molecule, to different paraffins within one channel, to interactions between paraffins in different channels, and to interactions between the paraffins and the urea host. The non-matching symmetry of the paraffins (orthorhombic) and the surrounding matrix (pseudo-hexagonal) is one source of a competing order behaviour giving rise to mutual distortions. Due to the non-matching c-periods of host and guest structures, there are commensuration problems along the unique direction. Apparently, the dynamics of (parts of) the paraffin molecules play a decisive role for order/disorder processes and subsequent phase transitions. Therefore, the diffuse scattering is highly temperature dependent and is closely related to different phase transitions which, however, depend sensitively on the type of paraffin molecule included. We have investigated inclusion compounds with hexa-, penta-, tri- and dodecane (Forst, 1984; Weber, 1994; Honal, 1994) and found similarities as well as significant differences in the diffuse scattering. Summarizing, very briefly, some of the common phenomena, there are (*cf.* Figs. 6*a* and *b*):

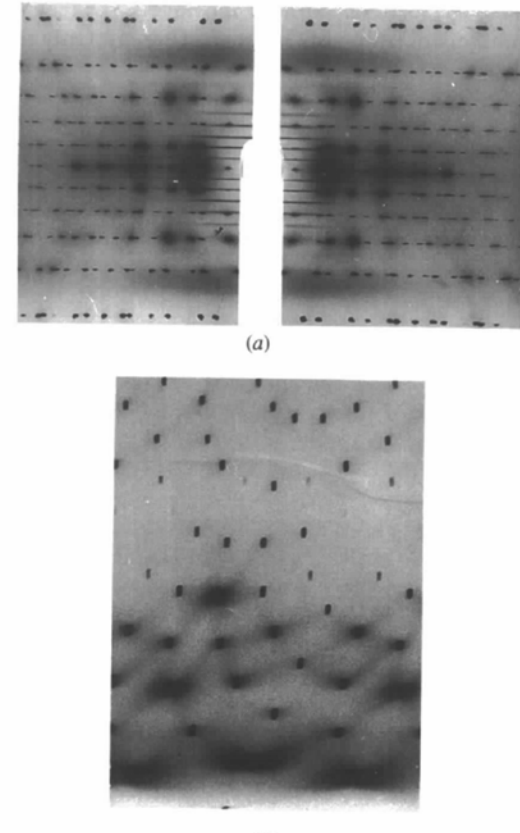

(*a*)

(*b*)

Fig. 6. UIC with hexadecane adduct: (*a*) Oscillation photograph around the c axis: ±30°, Cu $K\alpha$ radiation, Ge(111) monochromator, normal beam technique. The tiny lines close to the meridian (around the shadow of the crystal support) are the diffuse s layers, the broad diffuse bands close to the fourth Bragg layers are the d bands. (*b*) Weissenberg photograph of the $hk0$ layer, Cu $K\alpha$ radiation; diffuse streaking within the ($hk0$) plane. Both figures are taken from Forst *et al.* (1987). For further explanations, see text.

(i) A prominent set of fine diffuse layers ('*s* layers') perpendicular to the unique direction, which can be understood by a one-dimensional ordering of rotationally average paraffins within one channel and the disorder between the channels.

(ii) A second system of broad diffuse layers ('*d* bands') which can be related to a intrachain disorder, *i.e.* within one channel. The intensities of the *s* and *d* layers can be analysed in a semi-quantitative way (Forst, Jagodzinski, Boysen & Frey, 1987)

$$|\langle F\rangle|^2 = G^2(l')L^2(l')4f_c^2 1/9\cos^2\{2\pi l'z'\} \times [\cos 2\pi hx + \cos 2\pi ky + \cos 2\pi(h+k)z]^2$$

$$\langle |F|^2\rangle = NL^2(l')4f_c^2[A\cos^2 2\pi l'z' + B\sin^2 2\pi l'z'],$$

with $f_c =$ atomic form factor of C (hydrogens are neglected)

$$A = 1/3\{\cos^2 2\pi hx + \cos^2 2\pi kx + \cos^2 2\pi(h+k)x\},$$

$$B = 1/3\{\sin^2 2\pi hx + \sin^2 2\pi kx + \sin^2 2\pi(h+k)x\}.$$

$G(l')$ denotes the one-dimensional lattice function and $L(l')$ the Laue function of one paraffin molecule:

$$L(l') = \sin\{\pi 8c''/c'l'\}/\sin\{\pi c''/c'l'\},$$

c'' and c' refer to the c period of the C—C—C unit within one molecule and to the c period along the chain within a channel, respectively. $\langle F\rangle$ governs the intensity of the *s* layers, $\Delta F^2 = \langle |F|^2\rangle - |\langle F\rangle^2|$ of the *d* layers. Neutron diffraction experiments yield information regarding the significant contribution of the H-atoms and the (quasi-) elastic nature of the *d*-band scattering indicating a (quasi-) static origin of the disorder element;

(iii) A strange arrangement of curved streaks within the (*hk*0) plane, which are extended also along the c' direction. A simple qualitative explanation is that the effect is due to lamellar precursor domains existing within an otherwise orientationally disordered room-temperature phase (Fig. 7). Cooling down to low temperatures we have a phase transition to a pseudo-orthorhombic domain structure (Fig. 8). The phase transition is due to a lateral orientational order of *n*-alkanes in adjacent channels with a subsequent rhombic distortion of the urea host structure (Forst, Boysen, Frey, Jagodzinski & Zeyen, 1986). The transition is driven by freezing of dynamic processes (reorientational jump-diffusion of the chain molecules), which were studied by inelastic and quasielastic neutron scattering investigations (Boysen, Frey & Blank, 1988). There are remarkable differences between odd- and even-membered chains in the UIC (El Baghdadi, Guilleaume, Boysen, Dianoux & Coddens, 1994). For example, the transition is sharply defined in UIC with hexadecane, but extends over a wide temperature range in UIC with pentadecane (Weber, 1994). Fig. 9 shows the example with hexadecane: this is a variety of satellite scattering related either to the specific paraffin substructure or to the host structure. Qualitative explanations can be given by competing interactions and commensuration problems becoming dominant over the dynamic (motional) processes: the 'host' is highly deformed into a very complicated domain structure, while the paraffin chain system becomes the dominant part. Possibly the more correct term of UIC structures at low temperatures should then be read as 'paraffin enclosure compounds'.

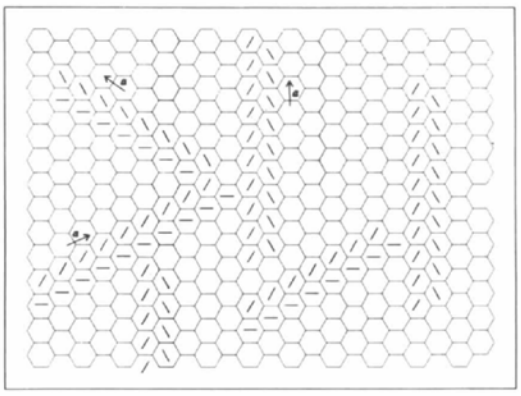

Fig. 7. Preformed lamellar precursor regimes in an otherwise orientationally disordered room-temperature phase of UIC (from Weber, 1994): the short lines in the honeycomb pattern indicate the orientations of the *n*-alkane molecules included in the channels. Empty channels indicate orientationally disordered molecules.

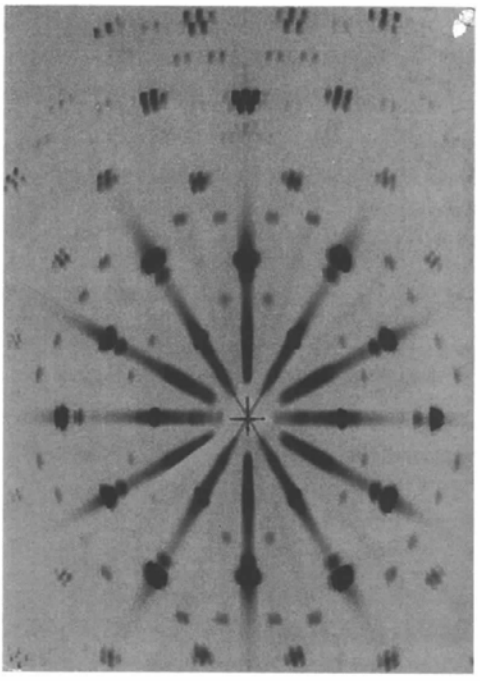

Fig. 8. X-ray precession photograph of the (*hk*0) plane of the low-temperature phase ($T \leq 148$ K) of UIC with a hexadecane adduct (Cu $K\alpha$ radiation). Note the ('lateral') splitting of the Bragg reflections, which is due to three pairs of orthorhombic domains (from Forst, Jagodzinski, Boysen & Frey, 1990).

This example demonstrated that (i) the temperature change is most helpful to differentiate between different diffuse scattering phenomena, (ii) both complementary X-ray and neutron scattering experiments are necessary to contrast different contributions of the constituents (C, O, N and H atoms), and (iii) inelastic and quasielastic neutron work is necessary to clarify the origin of diffuse scattering and, in consequence, to understand the role of the dynamics in a disorder problem.

4. Zirconia $ZrO_2(+CaO,Y_2O_3)$: microdomains and material properties

Zirconia exist in different polymorph structures which may be described by more or less distorted fluorite structures. We focus on the so-called cubic-stabilized zirconia. By adding oxides such as CaO or Y_2O_3, the high-temperature polymorph of pure ZrO_2, which has an undistorted fluorite structure, may be stabilized at room temperature. This is true as long as only the averaged structure is considered. Knowledge of the averaged structure is not enough, however, to understand the properties of this extremely important material. Only a detailed investigation of the defect structures, which depend on many factors such as particle size effects, exact stoichiometry, sample prehistory *etc.*, provides some insight. There is a vast literature about defects, disorder and diffuse scattering in zirconia, *e.g.* Heuer & Hobbs (1981), Claussen, Rühle & Heuer (1983), Chan (1986), Meriani & Palmonari (1988), and Sorrell & Ben-Nissan (1988). Fig. 10(*a*) (Neder, Frey & Schulz, 1990) shows a neutron diffraction pattern (purely elastic data) and Fig. 10(*b*) (Proffen, unpublished) an X-ray pattern, of the [110] zone of ZrO_2 stabilized with 15 mol % CaO. From these observations we learn that the disorder is mainly of static origin and both cations and oxygens contribute to the diffuse scattering. On both pictures two prominent diffuse features are clearly to be seen: diffuse maxima at regular distances from the Bragg peaks (diffuse satellites) and broad diffuse bands. These features were interpreted in terms of correlated and uncorrelated defect clusters by Neder, Frey & Schulz (1990). Equivalent patterns of zirconia stabilized with 21 mol % Y_2O_3 show similar phenomena in the neutron case. In the X-ray case, where Y and Zr have almost equal scattering power, there are different, partly controversial observations which might be due to different sample material (homogeneity!), but are still

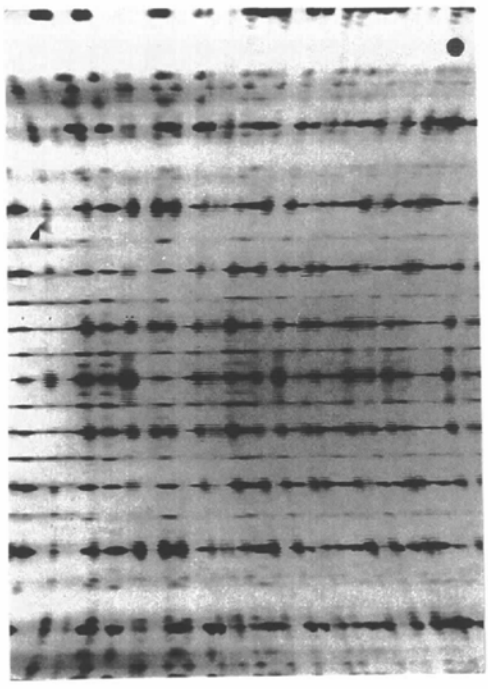

Fig. 9. Oscillation photograph as in Fig. 6, taken at 32 K (magnified section). The former *s* and *d* layers break up into Bragg peaks, indicating a three-dimensional ordering between the *n*-alkane molecules. Note also that some of the original Bragg reflections are split into a series of satellite reflections (along c*), indicating a complicated domain structure (from Forst *et al.*, 1987).

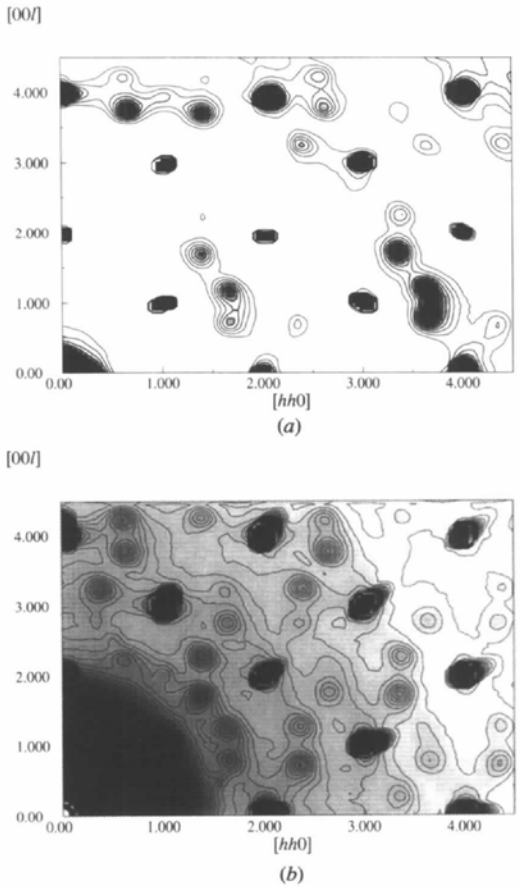

Fig. 10. Zirconia, ZrO_2 doped with 15 mol % CaO: Diffuse scattering in [110] zone. (*a*) Neutron scattering (wavelength 1.08 Å), from Neder *et al.* (1990); (*b*) X-ray scattering (Mo$K\alpha$ radiation, Proffen, unpublished). The positions of the Bragg peaks are marked by the black boxes.

under debate. Nevertheless, complementary X-ray and neutron investigations help to understand the relative contributions of the metal and the oxygen ions. The mobility of the oxygens controls the ionic conductivity of zirconia, which is important for its use at elevated temperatures as sensors or in fuel cells. *In situ* high-temperature diffraction investigations, in oxidizing or in reducing atmosphere, provide information regarding the change of the diffuse intensity and subsequently give insight into the evolution of the corresponding defect clusters and the correlations between them. Fig. 11 (Proffen, Neder, Frey, Keen & Zeyen, 1993) shows, for example, the temperature evolution of the diffuse scattering in ZrO_2+10 and 15 mol% CaO. It was concluded that the correlation lengths between the defect clusters are independent of concentration and temperature, the relative amount of uncorrelated to correlated microdomains, however, changes in favour of uncorrelated ones. This result may be discussed in connection with the increased ionic conductivity. Thus, structural information obtained from diffuse data helps one to understand how material properties depend on the stoichiometry, the actual temperature, the surrounding atmosphere, and further parameters such as sintering conditions. The last remarks points towards a new wide field of diffuse scattering investigations on powdered samples which is not considered in this overview.

5. Decagonal phase $Al_{70}Ni_{15}Co_{15}$: disorder in quasicrystals

Investigations of disorder in quasicrystals are relatively new; an elementary introduction into diffraction by quasicrystals is given by Janot (1992). To illustrate disorder diffuse scattering from quasicrystals we take as an example decagonal $Al_{70}Ni_{15}Co_{15}$ (*d*-ANC), which is a two-dimensional quasicrystal ($N = 5$) with translational order along the remaining direction. The most significant structural elements of the average structure of *d*-ANC are columns and clusters of columns parallel to the unique direction. The space group is $P10_5/mmc$ (Steurer, Haibach, Zhang, Kek & Lück, 1993). *d*-ANC has a repeat distance of approximately 4 Å in the periodic direction. Within this period there are two equivalent structural units rotated by 36° with respect to one another. There is a super-ordering element with doubling of this period. From our observations were conclude that this super-ordering is a characteristic feature of *d*-ANC and other isotypic decagonal phases, in agreement with the observations of Hiraga, Lincoln & Sun (1991) and Edagawa, Ichihara, Suzuki & Takeuchi (1992). More structural details of the averaged structure of *d*-ANC are given by Steurer *et al.* (1993). The phase is reported to be thermodynamically stable above 773 K (Tsai, Inoue & Masumoto, 1989). Daulton & Kelton (1992) report strong diffuse intensity and spot-shape anisotropy in selected area electron-diffraction patterns. The existence of a true decagonal twinned microcrystalline modulated q.c. phase is still under debate for ANC of virtually the same chemical composition. The prehistory of a sample, *i.e.* the temperature–time treatment, annealing, irradiation, play a decisive role for various disorder phenomena, including glass-like phases. Rational crystalline 'approximant' phases are also reported (Hiraga *et al.*, 1991). In our experimental work (Frey & Steurer, 1993; Hradil, Proffen, Frey, Kek, Krane & Wroblewski, 1995; Hradil, Proffen, Frey, Eichhorn & Kek, 1995) we found a variety of puzzling diffuse phenomena with highly anisotropic distribution in reciprocal space. Their intensities change with small variations of exact stoichiometry and other factors. In order to characterize the diffuse phenomena high-intensity and high-resolution methods are necessary and only the combination of different methods offers a chance of solving the disorder problems.

Summarizing in brief the most prominent diffuse scattering phenomena, we have (Fig. 12*a*):

(i) Diffuse layers perpendicular to the unique (tenfold) axis halfway between a set of Bragg layers which reflect, to a first approximation, uncorrelated one-dimensional long-range ordered columns with a doubled period parallel to the unique direction. *In situ* high-temperature investigations show a gradual decrease of this super-ordering, which vanishes at *ca* 1073 K. This process is fully reversible.

(ii) Diffuse modulations within the diffuse layers (Fig. 12*b*). This indicates that there are lateral short-range (60 Å) correlations between the super-periodically ordered columns. This short-range order has a different symmetry from that of the average structure. These modulations become unobservable with decreasing intensity of the diffuse layers (i).

(iii) Diffuse satellite scattering ($\mathbf{q}_s$) (Fig. 12*c*).

(iv) Diffuse streaks (Fig. 12*c*).

(v) Diffuse pentagons within the Bragg layers (Fig. 12*c*).

Figs. 13(*a*), (*b*) and (*c*) show the phenomena (iii)–(v) in more detail. The satellite positions can be indexed by commensurate values $(\frac{1}{8}, \frac{2}{8})$. The diffuse streaks and the

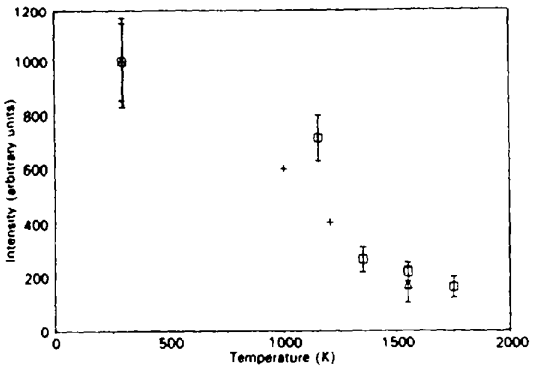

Fig. 11. As Fig. 10: Temperature dependence of a diffuse maximum (neutron work). Differently labelled points refer to different experiments at different neutron sources (*cf.* Proffen *et al.*, 1993).

satellite reflections are strong around strong Bragg reflections and show no remarkable **Q**-dependence. Both phenomena have the same structure origin. From this streaking we deduce that there are layer-like blocks which are extended along the unique (= periodic) direction. The correlation length along this direction exceeds 1000 Å and matches that of the basic averaged substructure. From a recent experiment on a synchrotron source we know that this lower limit is even as high as 10 000 Å. The extension of the blocks in the perpendicular direction and along the stacking direction are of the order 200 Å. The existence of satellite scattering proves there is pronounced super-ordering. From the commensurability of the $\mathbf{q}_s$ vectors we have a translational superperiod of 30 Å, the average correlation length corresponds to 6–7 supercells. Many faults, however, interrupt this stacking. These layer-like blocks are arranged in such a way that the overall point symmetry 10 *mm* is preserved. The 30 Å period may be easily related to one pair of inflated fat and skinny tiles (Fig. 14; for a discussion of inflation see Janot, 1992). There are different possible interpretations, such as:

(i) a translational superperiod is superimposed on a quasiperiodic substructure;

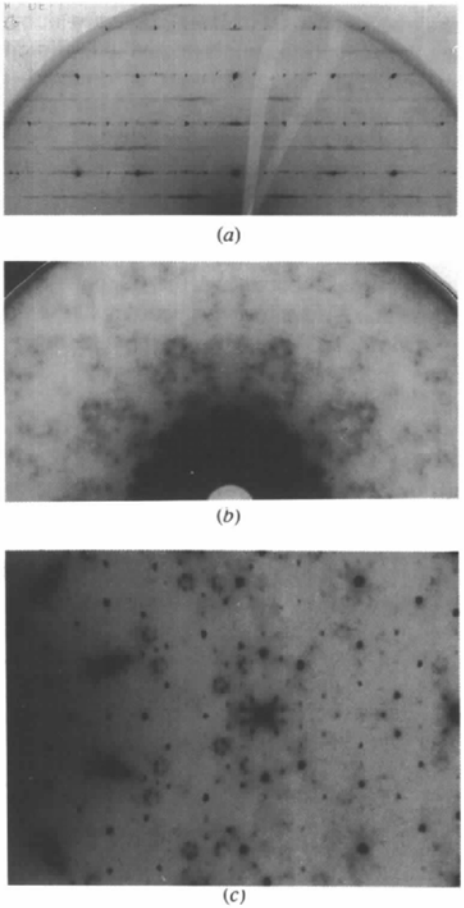

(*a*)

(*b*)

(*c*)

Fig. 12. Precession photographs of decagonal *d*-ANC (Mo$K\alpha$ radiation): Layer line system perpendicular to the unique axis (periodic direction); the abscissa is any direction in the quasiperiodic plane. Note the sequence of diffuse layers corresponding to a double period (*a*); first diffuse layer [*cf.* (*a*)]: short-range modulations are clearly visible (*b*); zero Bragg layer: note the short diffuse streaking and superimposed satellite scattering close to strong reflections as well as small diffuse 'pentagons' (*c*).

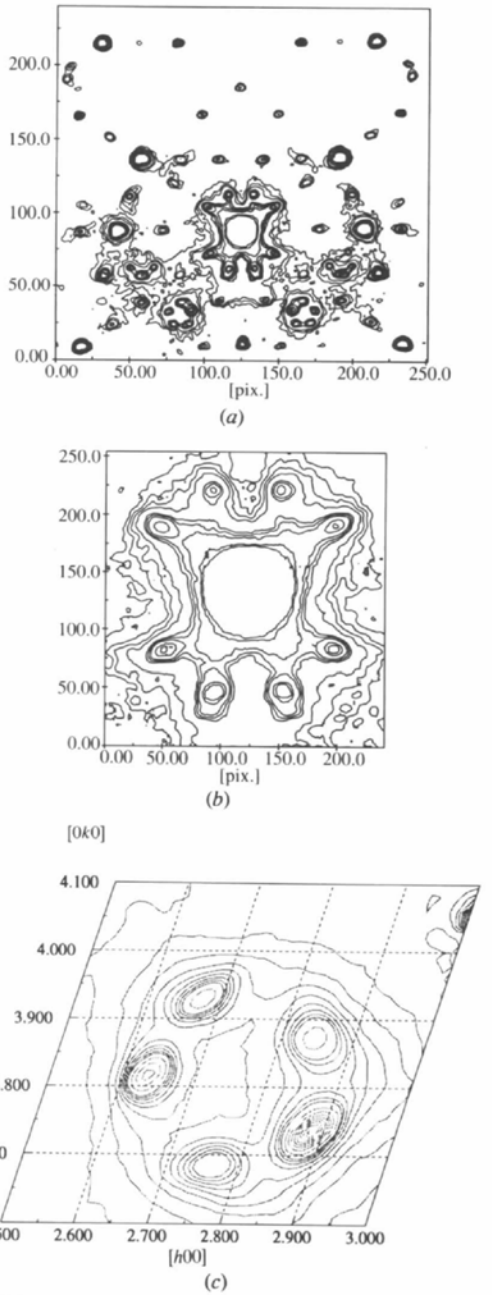

Fig. 13. Enlarged section from Fig. 12(*c*), $Al_{70}Ni_{15}CO_{15}$ zero layer, obtained by a flat bed scanner (Proffen & Hradil, 1993): (*a*) streaks and satellites close to Bragg reflections; (*b*) enlarged section from (*a*): Bragg spot, diffuse streaks, and diffuse satellites; (*c*) diffuse pentagon [*cf.* (*a*) and Fig. 12(*c*)] measured at the diffractometer D3 of the synchrotron source DESY/Hamburg (Hradil, Proffen, Frey, Eichhorn *et al.*, 1995).

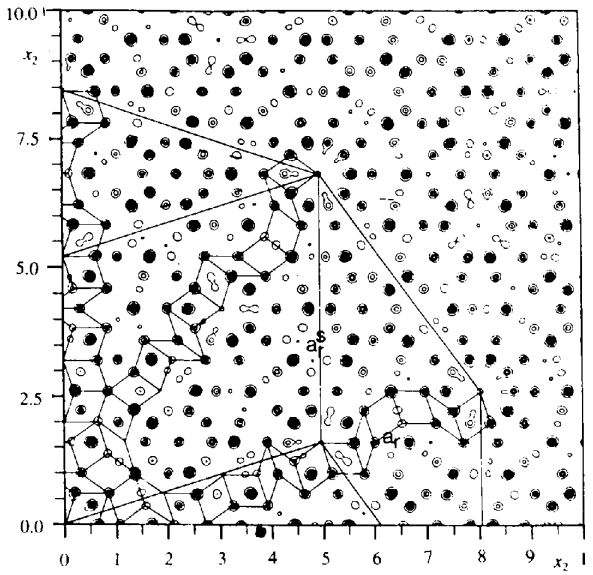

Fig. 14. Inflated fat and skinny tiles in the averaged quasiperiodic arrangement of *d*-ANC. Picture taken from Steurer *et al.* (1993), Fig. 8(*b*) therein. 'Inflation' indicates a scaling with powers of τ (the golden mean). For further explanation, see *e.g.* Janot (1992) and the original literature.

(ii) quasiperiodic domains are separated by periodically ordered domains [approximant(s)]; with a, more or less well defined, superperiod of 30 Å;

(iii) twinned microcrystalline domains are intergrown with an average overall tenfold symmetry and a superordering due to coherency strains.

Some of the models are schematically shown in Figs. 15(*a*)–(*f*), which are simple pictures in the frame of the superspace concept. More detailed information is given in the figure caption. In any case we have a complicated interplay and competition between crystallinity and quasicrystallinity. Note that sharp Bragg reflections always exist as long as coherence of a q.c. substructure persists across the domain/twin boundaries. The observations that the satellites and the diffuse streaks are only strong near strong Bragg reflections and have remarkable intensity at low scattering angles indicate a compositional component of the superperiodic ordering. From the existence of second-order satellites and the intensity ratio $I(2\mathbf{q}_s)/I(\mathbf{q}_s) \geq 1/2$, we conclude there is a need for an anharmonic asymmetric modulation function (Fig. 16). High-resolution electron microscope pictures of isotypic $Al_{65}Cu_{15}Co_{20}$ (Chen, Burkov, He, Poon & Shiflet, 1990) show features which can easily be understood in this

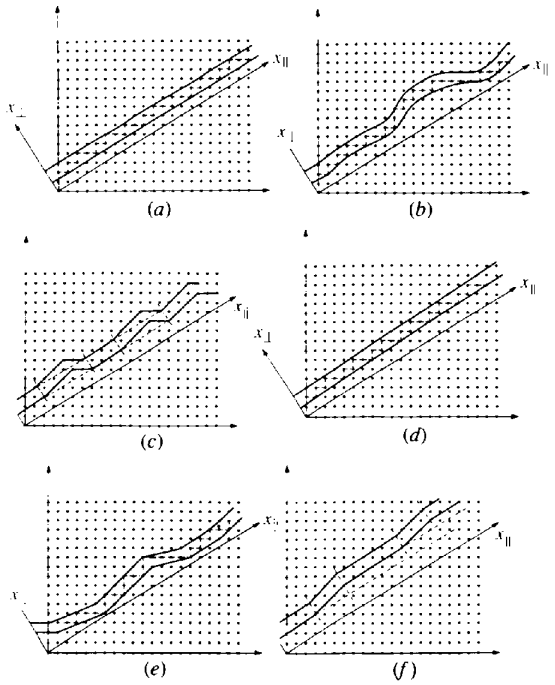

Fig. 15. Schematic pictures of a one-dimensional quasicrystal using the cut and project method in two-dimensional hyperspace (*cf.* Janot, 1992). $X_\parallel$ and $X_\perp$ denote the external (=real) and internal space, respectively: (*a*) undistorted Fibonacci sequence; (*b*) approximant phase; (*c*) phason strained quasicrystal produced by an unbounded meandering sequence; (*d*) intergrowth of microcrystalline approximant phases, note the stepwise commensurate slopes; (*e*) intergrowth of two microcrystalline approximants and a true quasicrystalline phase; (*f*) superperiodic sequence of an approximant and the q.c. phase: hypothetical case due to large phason stains. (*a*)-(*d*) redrawn from Fig. 8 of Goldman & Kelton (1993).

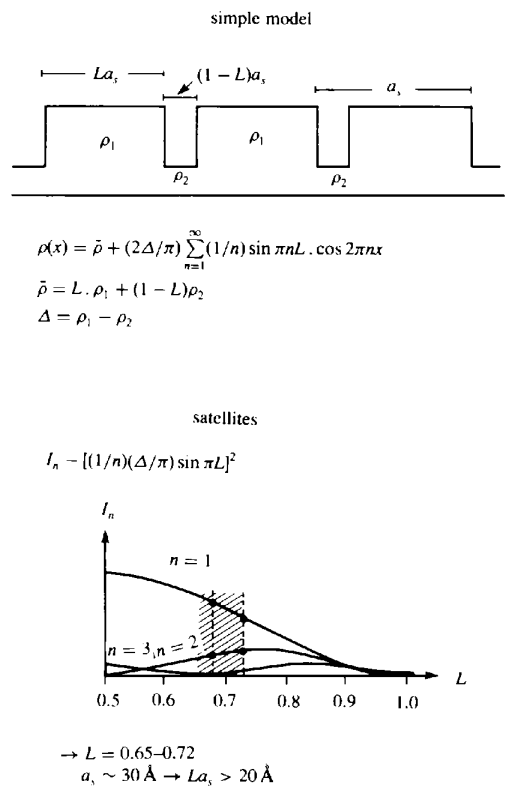

Fig. 16. Schematic picture of a strongly anharmonic asymmetric modulation function, *e.g.* a periodic sequence of two kind of domains of length L and $(1-L)$, respectively (above); intensity behaviour of corresponding satellite scattering (below): the parameter L governs the intensities I_n of the different orders of the satellite scattering (Fourier–Bessel functions; Korekawa, 1967).

way. Only a quantitative analysis of the diffuse scattering in combination with direct electron microscope observations seems to be promising to solve the problem. This is a task and challenge for future work.

Raising the temperature results in the diffuse streaks becoming weaker at 1123 K and then vanishing above 1148 K, which clearly proves their origin is different from that of the diffuse layers. The transitional processes within and between the complicated disordered and superordered quasiperiodic and periodic domain structures occur in a temperature regime where an increase of the thermodynamical stability of the *d*-ANC phase was reported (Kek, 1991). Further conclusions can now be drawn about the existence and stabilization of quasicrystalline phases for energetic or entropic reasons. This discussion is beyond the aim of this overview.

6. Concluding remarks and future trends

Disorder in any crystal is unavoidable for general physical reasons: $G = U - TS$ (usual meaning of the symbols). Corresponding investigations are important for both clarifying basic fundamental questions and for understanding material properties. The type and amount of disorder varies considerably from a defect-free perfect silicon specimen to, for example, mesophases or glass-like structures. Diffuse scattering investigations provide direct access to a disorder problem. If the key to an understanding of a structural order problem or a crystal property is the underlying disorder, the analysis of diffuse scattering provides an invaluable tool often to be complemented by other methods. The experimental situation requires and can be improved by the development of new methods, *e.g.* dedicated instruments at powerful synchrotron sources (Rosshirt, Frey, Kupcik & Miehe, 1990). The intense beams, tight collimations and the tuneable wavelength of these sources allow for high-resolution experiments up to high scattering angles and to distinguish the atoms which are responsible for an underlying disorder problem. Enhanced use of area detectors allows for simultaneous recording of large areas of reciprocal space. The essential background problem could be overcome – at least partly – by setting a complete diffractometer in an evacuated hutch. The availability of a microfocus-beam could close a gap: the same part of a sample and, therefore, the same disorder phenomenon could be attacked by scattering methds with high resolution and compared with direct images (electron microscopy). Then, X-ray diffraction patterns and direct electron microscope observations can be safely compared and may be used in a complementary way. Neutron work is absolutely necessary to enhance the relative scattering power of the light elements or to clarify the static and/or dynamic origin of the disorder problem.

This work was supported by funds of the BMFT and of the DFG of Germany.

Reference

BOYSEN, H. & ADLHART, W. (1987). *J. Appl. Cryst.* **20**, 200–209.

BOYSEN, H., FREY, F. & BLANK, H. (1988). *Mater. Sci. Forum*, **27/28**, 123–128.

CHAN, S. K. (1986). Proc. Int. Conf. Zirconia '86. Tokyo.

CHEN, H., BURKOV, S. E., HE, Y., POON, S. & SHIFLET, G. J. (1990). *Phys. Rev. Lett.* **65**, 72–75.

CLAUSSEN, N., RÜHLE, M. & HEUER, A. H. (1983). *Advances in Ceramics*, Vol. 12. Columbus: American Ceramics Society.

DAULTON, T. L. & KELTON, R. F. (1992). *Philos. Mag. B*, **66**, 37–61.

EDAGAWA, K., ICHIHARA, M., SUZUKI, K. & TAKEUCHI, S. (1992). *Philos. Mag. Lett.* **66**, 19–25.

EL BAGHDADI, A., GUILLEAUME, F., BOYSEN, H., DIANOUX, A. J. & CODDENS, G. (1994). *QENS'93: Quasielastic Neutron Scattering*, pp. 131–140. Singapore: World Scientific.

ENDRES, H., HARMS, R., KELLER, H. J., MORONI, W., NÖTHE, P., VARTANIAN, M. H. & SOOS, Z. G. (1979). *J. Phys. Chem. Solids*, **40**, 591–596.

FORST, R. (1984). PhD Thesis. LMU, München, Germany.

FORST, R., BOYSEN, H., FREY, F., JAGODZINSKI, H. & ZEYEN, C. (1986). *J. Phys. Chem. Solids*, **47**, 1089–1097.

FORST, R., JAGODZINSKI, H., BOYSEN, H. & FREY, F. (1987). *Acta Cryst.* B**43**, 187–197.

FORST, R., JAGODZINSKI, H., BOYSEN, H. & FREY, F. (1990). *Acta Cryst.* B**46**, 70–78.

FREY, F. & STEURER, W. (1993). *J. Non-cryst. Solids*, **153/154**, 600–605.

FUKAO, K. (1994). *J. Chem. Phys.* **101**, 7882–7892, 7893–7903.

GOLDMAN, A. I. & KELTON, K. F. (1993). *Rev. Mod. Phys.* **65**, 213–230.

HARRIS, K. D. M. (1993). *J. Solid State Chem.* **106**, 83–98.

HEUER, A. H. & HOBBS, L. W. (editors) (1981). *Advances in Ceramics*, Vol. 3. Columbus: American Ceramics Society.

HIRAGA, K., LINCOLN, F. J. & SUN, W. (1991). *Mater. Trans. Jpn Inst. Met.* **4**, 308–314.

HONAL, M. (1994). Diploma Thesis. LMU, München, Germany.

HOSEMANN, R. & BAGCHI, S. N. (1962). *Direct Analysis of Diffraction by Matter*. Amsterdam: North-Holland.

HRADIL, K., PROFFEN, T., FREY, F., EICHHORN, K. & KEK, S. (1995). *Philos. Mag Lett.* **71**, 199–205.

HRADIL, K., PROFFEN, T., FREY, F., KEK, S., KRANE, H. G. & WROBLEWSKI, T. (1995). *Philos. Mag. A*. In the press.

JAGODZINSKI, H. (1964). *Advances in Structural Research*, edited by R. BRILL & R. MASON, Vol. 1, pp. 167–198. Braunschweig: Vieweg.

JAGODZINSKI, H. (1987). *Progress in Crystal Growth and Characterization*, edited by P. KRISHNA, pp. 47–102. Oxford: Pergamon Press.

JAGODZINSKI, H. & FREY, F. (1993). *International Tables for Crystallography*, edited by U. SHMUELI, Vol. B, ch. 4.2, pp. 392–433. Dordrecht: Kluwer Academic Publishers.

JANOT, C. (1992). *Quasicrystals – A Primer*. Oxford: Clarendon Press.

JARIC, M. V. & NELSON, D. R. (1988). *Phys. Rev. B*, **37**, 4458–4472.

KEK, S. (1991). PhD Thesis. Univ of Stuttgart, Germany.

KOREKAWA, M. (1967). Habilitation Thesis, Univ. of München, Germany.

MERIANI, S. & PALMONARI, C. (1988). Proc. Int. Conf. Zirconia '88. Blogna. Amsterdam: Elsevier Science.

MILLANE, R. P. (1989). *Acta Cryst.* A**45**, 258–260.

NEDER, R., FREY, F. & SCHULZ, H. (1990). *Acta Cryst.* A**46**, 799–809.

PROFFEN, TH. & HRADIL, K. (1993). *Z. Kristallogr.* Suppl. 7, 155.

PROFFEN, TH., NEDER, R., FREY, F., KEEN, D. A. & ZEYEN, C. (1993). *Acta Cryst.* B**49**, 605–610.

ROSSHIRT, E., FREY, F., BOYSEN, H. & JAGODZINSKI, H. (1985). *Acta Cryst.* B**41**, 66–76.

ROSSHIRT, E., FREY, F., KUPCIK, V. & MIEHE, G. (1990). *J. Appl. Cryst.* **23**, 21–25.

SORRELL, C. C. & BEN-NISSAN, B. (editors) (1988). *Mat. Sci. Forum*, **34/36**, ch. 2.

STEURER, W., HAIBACH, T., ZHANG, B., KEK, S. & LÜCK, R. (1993). *Acta Cryst.* B**49**, 661–675.

STUBBS, G. (1989). *Acta Cryst.* A**45**, 254–258.

TSAI, A. P., INOUE, A. & MASUMOTO, T. (1989). *Mater. Trans.* **30**, 463–473.
WEBER, T. (1994). Diploma Thesis. LMU, München, Germany.
WELBERRY, T. R. (1985). *Rep. Prog. Phys.* **48**, 1543–1593.
WELBERRY, T. R. & BUTLER, B. D. (1994). *J. Appl. Cryst.* **27**, 205–231.
WILDGRUBER, U. (1989). PhD Thesis. LMU, München, Germany.